

A Novel High-Gain Circularly Polarized Omnidirectional Filtenna Based on Coaxial Structure

Duo ZHAN¹, Keren ZHU², Shishan QI²

¹Dept. of Nanjing Institute of Technology, 211167 Nanjing, China

²Dept. of School of Electronic Engineering and Optoelectronic Technology, Nanjing University of Science and Technology, Xiao Ling Wei 200#, 210094 Nanjing, China

duozhang@njit.edu.cn, kerenzhu@gmail.com, qishishan@gmail.com

Submitted January 21, 2025 / Accepted May 5, 2025 / Online first June 12, 2025

Abstract. A novel omnidirectional slot array filtenna with a circularly polarized (CP) radiation beam is presented in this paper. This filtenna utilizes the coaxial cylinder structure, and the antenna's filtering function is primarily achieved through the direct synthesis method of a tubular bandpass filter. Four perpendicular slot pairs form the basic omnidirectional CP radiation element, which is cut into the sleeve and added to the outer conductor of the coaxial cylinder to implement the compact performance. To simplify the design, this work utilizes the high and low impedance conversion of the inner conductor, as well as isolation through dielectric materials. This filtenna achieves high gain by forming an array along the z -axis direction and placing the antenna elements reasonably for radiation in phase. A prototype was designed and fabricated to validate its practicality. The results indicate a fractional impedance bandwidth ($S_{11} < -10$ dB) of 5.8%, from 8.87 to 9.39 GHz, and a 3-dB axial-ratio (AR) bandwidth of 6.1%, from 8.85 to 9.40 GHz. The realized gain of the antenna is consistently higher than 5.29 dBi over the operating bandwidth, and its out-of-roundness is less than 1.5 dB in the radiation direction.

filtering response are widely utilized in radio and television broadcasting, mobile communication, indoor distribution systems, vehicle stations, satellite communication, and various modern wireless communication systems [13].

In recent years, various resonant filters, such as loop-resonator filters, step-impedance resonators and quarter-wavelength resonator filters, have been employed to excite monopole and dipole antennas resulting in satisfactory filtering characteristics [14–21]. To reduce insertion loss, the work proposed in [22] incorporates non-radiating elements, including a coupled U-shaped microstrip line and two I-shaped slots both located in the feeding network, to achieve filtering performance. However, it only achieves a gain of 2.5 dBi. The filtennas based on dielectric resonator structures are investigated in [23–25] but they face the same issue of low gain.

Recently, a triangular patch antenna has been excited in both its TM_{01} and TM_{11} modes, achieving a filtering response through the combination of a ring slot and a series of shorting vias introduced onto the patch [26]. However,

Keywords

Circular polarized (CP) filtenna, filtering antenna, axial ratio (AR), omnidirectional antenna, tubular bandpass filter

1. Introduction

Due to the 360° full-signal coverage, low multipath reflections, and absences of polarization mismatches, omnidirectional circularly polarized (CP) antennas have increasingly attracted the attention of researchers. Traditional designs for realizing omnidirectional antennas include dipole antennas [1–3], loop antennas [4], [5], microstrip patch antennas [6–8], and slot antennas [9], [10]. Furthermore, owing to their compact size and low insertion loss [11], [12], CP omnidirectional antennas with integrated

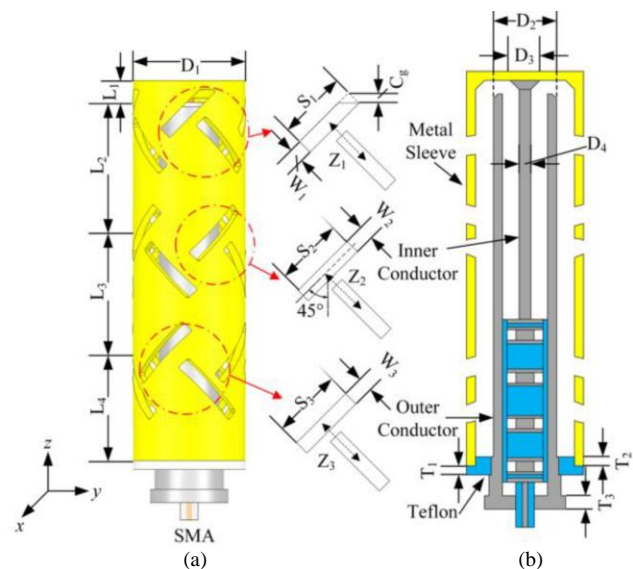


Fig. 1. Geometry of the omnidirectional filtenna. (a) Side view. (b) Cross-sectional view.

the filtenna has a considerable size, measuring $1.45\lambda_0 \times 1.45\lambda_0$, due to its large ground area. Meanwhile, typical low-profile omnidirectional filtennas are linearly polarized. Additionally, their operating bands are confined to the S-band and C-band, lacking the capability to expand to higher frequencies, which makes them difficult to be applied to X-band communication systems. A compact wideband circularly polarized planar filtenna has been proposed in [27] which combines a hairpin line filter and a hexagonal shaped CP antenna element. However, the cross-pol of the design is inconsistent across the entire plane. Similarly, cascaded filter structures and radiation structures are employed to implement wideband linearly polarized monopole and dipole filtennas in [28], [29]. Due to the cascaded structure, the filter and antenna occupy space solely which is difficult to implement compact performance. CP horn antennas with good filtering performance have been proposed in [34], [35]. Although the pencil beams are generated, the method of achieving circular polarization is quite ingenious. In [36], a compact polarization rotator is designed to replace the traditional polarization-twisting device. In [37], a compact filtering antenna using composite right/left-handed (CRLH) transmission line structure is presented. Series LC and parallel LC circuits are employed to generate radiation nulls. Full-Metal omnidirectional filtenna array using 3-D metal printing technology is designed in [38]. The polarization of this design is linear. Due to the poor surface roughness of 3D-printed structures, antenna losses will increase at high frequencies.

In this paper, CP omnidirectional radiation is achieved using an all-metal coaxial waveguide structure with three sets of perpendicular slot pairs cut into the external metal sleeve, which is connected to the inner conductor, as illustrated in Fig. 1. In fact, the integrated filtering function into a waveguide slot array antenna is very difficult. Even minor modifications can significantly affect the radiation performance of a series-fed waveguide array. By integrating the filter into the inner conductor of the coaxial waveguide, the antenna's compact size can be maintained without compromising its radiation characteristics. The method proposed in this paper represents the optimal solution for designing filtered waveguide slot antenna arrays. This design approach ensures that the filtering characteristics and radiation properties can be independently optimized without mutual interference. According to previous literature, a filtering response has not been realized on this structure before [30], [31]. Therefore, the proposed antenna creatively utilizes the impedance transformation of the inner conductor of the coaxial waveguide and incorporates dielectric discs into the structure to achieve a filtered response. Specifically, the filtenna employs a simpler and more precise design methodology based on S-parameter curve-fitting to obtain a bandpass filtering function [32], [33]. A prototype operating at 9 GHz was optimized and fabricated. This design eliminates the need for a complex feed network, offers higher gain, and provides significant advantages in terms of horizontal dimen-

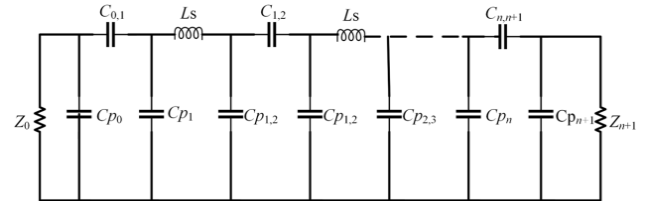


Fig. 2. Circuit diagram of the narrowband bandpass filter.

sions compared to existing planar omnidirectional filtennas. Additionally, it uses a nested coaxial structure to achieve a more compact structure and easier processing compared to antennas with conventional metallic circular waveguide structures.

2. Design of Filter

Before presenting the integrated filtenna, a four-order tubular bandpass filter is designed, as shown in Fig. 2. Tubular filters have been extensively studied in wireless communication due to their advantages of compact structure, low insertion loss, and high-power capacity. The topology is typically derived from K -impedance converter theory and consists of Π -resonator capacitor networks and series inductors that are alternately cascaded. The filter operates at 9 GHz with a fractional bandwidth (FBW) of 4.8%, ranging from 8.79 GHz to 9.22 GHz.

First, it is essential to determine the inductance based on the operating frequency, taking $L_s = 0.3$ nH (all inductors are equal in value). The capacitance values C_{p0} , $C_{0,1}$ and C_{p1} at the source, as well as the capacitance in series between neighboring inductors of the filter, are determined by the following equation[32, 33].

$$C_{0,1} = \sqrt{\frac{G'_0(1 + Z'_0 \omega_0^2 Cx_0^2)}{Z_0 \omega_0^2}}, \quad (1)$$

$$C_{p0} = Cx_0 - C_{0,1}, \quad (2)$$

$$C_{p1} = \frac{1}{\omega_0} \left[B'_0 - \frac{\omega_0 C_{0,1} (1 + Z'_0 \omega_0^2 C_{p1} Cx_0)}{1 + (Z_0 \omega_0 Cx_0)^2} \right], \quad (3)$$

$$C_{i,i+1} = \frac{[2C_s / (1 - 2C_s \omega_0 K_{i,i+1})]^2}{4C_s / (1 - 2C_s \omega_0 K_{i,i+1}) + 1/\omega_0 K_{i,i+1}}, \quad (4)$$

$$C_{p_{i,i+1}} = \frac{[2C_s / (1 - 2C_s \omega_0 K_{i,i+1})] / \omega_0 K_{i,i+1}}{4C_s / (1 - 2C_s \omega_0 K_{i,i+1}) + 1/\omega_0 K_{i,i+1}} \quad (5)$$

where Cx_0 is introduced to ensure that the capacitance values of C_{p0} , $C_{0,1}$ and C_{p1} can be realized by a physical component, even though the values of the above capacitances are all positive. By empirical data, Cx_0 is generally chosen to ensure that $C_{p0} = C_{p1}$. The Cx_0 will finally be determined using a Python program to calculate the above equations. The values of G'_0 and B'_0 are calculated from (6) to (11) as follows:

$$G'_0 = \frac{Z_0(2\omega_0 C_S K_{0,1})^2}{Z_0^2 + (2\omega_0 C_S K_{0,1})^2}, \quad (6)$$

$$B'_0 = \frac{Z_0^2(2\omega_0 C_S)}{Z_0^2 + (2\omega_0 C_S K_{0,1})^2}, \quad (7)$$

$$C_S = \frac{1}{\omega_0^2 L_S}, \quad (8)$$

$$K_{0,1} = \sqrt{\frac{Z_0 \cdot \text{FBW} \cdot \omega_0 L_S}{\Omega_C g_0 g_1}}, \quad (9)$$

$$K_{i,i+1} = \frac{\text{FBW} \cdot \omega_0 L_S}{\Omega_C} \sqrt{\frac{1}{g_i g_{i+1}}}, \quad (i=1, 2, \dots, n-1), \quad (10)$$

$$K_{n,n+1} = \sqrt{\frac{Z_{n+1} \cdot \text{FBW} \cdot \omega_0 L_S}{\Omega_C g_n g_{n+1}}} \quad (11)$$

where the g_i and Ω_C are the original value and cut-off frequency of the n -order low-pass filter prototype, respectively.

The theoretical values of all capacitors are presented in Tab. 1. A thin high-impedance line can be directly utilized as a series inductor, while a ring disc serves as a series capacitor. Additionally, a low-impedance line can be employed using the outer conductor of the coaxial cylinder to form a parallel capacitor. The simulation results of the 3D structure using HFSS software are curve-fitted with the simulation results of the schematic circuit diagram using ADS software to extract the equivalent inductance and capacitance values corresponding to different structure dimensions in this design.

To enhance accuracy, it is essential to consider both the distributed capacitance effects of high impedance lines and the distributed inductance effects of low impedance lines. Additionally, the response remains nearly constant at the same single-cavity resonant frequency and the intercavity coupling coefficient for coupled resonant filters. The H-shape resonant units, which are independent of one another, are illustrated in Fig. 3 with the grey section representing the metal shell, the orange inner conductor, and the blue Teflon. They are selected as the simulation model and the simulation curves of their equivalent circuits serve as the target values.

The overall physical structure of the tubular filter is constructed based on this foundation and is shown in Fig. 4. After fine-tuning and optimization, the final filter dimensions

Symbol	Value	Symbol	Value
$C_{0,1}$	2.2848	C_{p1}	1.2658
$C_{1,2}$	0.1272	$C_{p1,2}$	1.9654
$C_{2,3}$	0.0976	$C_{p2,3}$	1.9918
$C_{3,4}$	0.1272	$C_{p3,4}$	1.9654
$C_{4,5}$	2.2848	C_{p4}	1.2658
C_{p0}	1.2152	C_{p5}	1.2152

Tab. 1. The theoretical values of all capacitors (in pF).

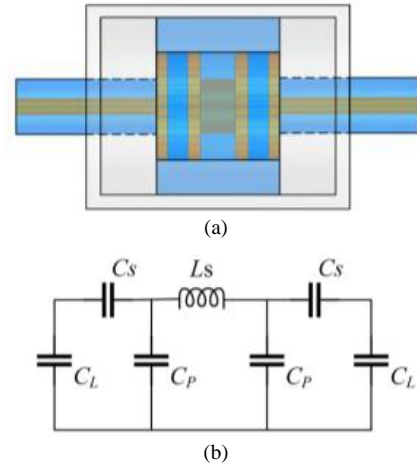


Fig. 3. H-shape resonant units. (a) Geometric structure. (b) Circuit diagram.

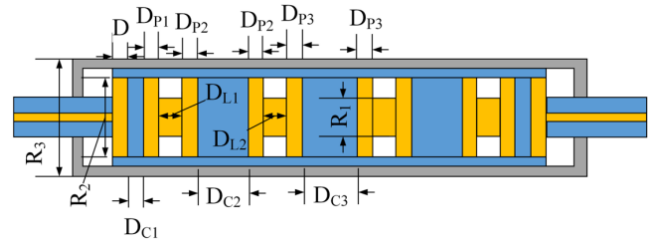


Fig. 4. Geometry of the coaxial tubular filter (The right dimension is symmetrical to the left).

Symbol	Value	Symbol	Value
R_1	8.0	DC_3	6.6
R_2	10.0	DP_1	0.6
R_3	12.0	DP_2	0.8
D	0.9	DP_3	0.6
DC_1	0.6	CL_1	2.3
DC_2	5.6	CL_2	2.3

Tab. 2. Optimized geometric parameter of the filter (in mm).

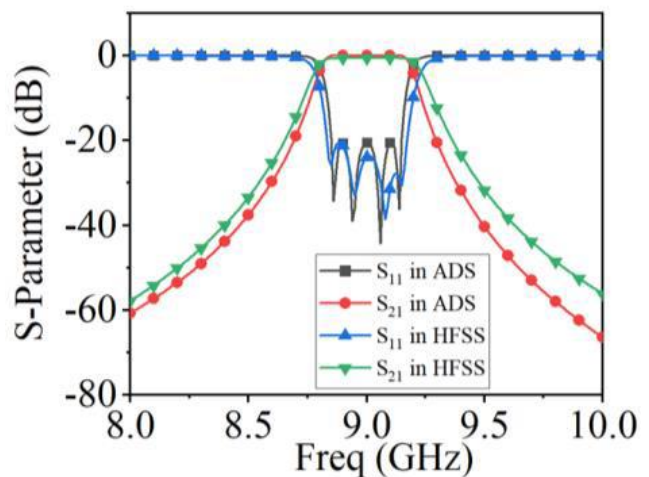


Fig. 5. Comparison of the simulated S-parameter in ADS and HFSS.

are shown in Tab. 2. The simulation results obtained by Ansoft HFSS, agree well with the theoretical values of the target circuit shown in Fig. 5.

3. Design of Filtenna

The complete filtenna is illustrated in Fig. 1 and the perpendicular slot pairs arrays in the outer conductor of the coaxial waveguide is designed to achieve the CP and omnidirectional performance. Additionally, a folded air-filled coaxial waveguide has been used as the feeding structure. The transition from the filter coaxial waveguide to the radiation coaxial waveguide is located at the top of the filtenna.

3.1 Design of Antenna

The radiating component of the antenna is constructed using the universal cut rectangular slots. Three sets of perpendicular slot pairs are cut into the surface of the sleeve, and one of the slots in each pair is inclined at a clockwise angle of 45° while the other leans at an anti-clockwise at 45°[30]. When the centers of the narrow radiating slots are appropriately optimized, they will then radiate circular or near-circular polarization waves. Also, the second set of slot pairs and the third set of slot pairs were rotated by 30° and 60° along the circumferential direction, respectively.

The length of each slot is approximately $\lambda_g/2$ (λ_g is the medium wavelength) and the distance between two slots is set to about $\lambda_g/4$ along the z-axis. This configuration is necessary to achieve left-hand circularly polarized (LHCP) characteristics, as it requires the waves excited from the slot pairs to have a 90° phase difference. The simulated electric field distribution on the sleeve at 9 GHz is illustrated at different time instants in Fig. 6. The three sets of slot pairs are arranged along the z-axis to form slot arrays to enhance gain. Each slot pair is positioned at intervals of $L_2 = L_3 = \lambda_g$ to ensure that the waves excited from them are in phase. The antenna has the property of omnidirectional radiation in the xoy plane, and its gain can be improved by adjusting the spacing of the slot pairs to be approximately equal to the free space wavelength in the z-axis direction. Specifically, the slot array elements closest to the upper surface are cut to a length of C_g compared to the others to eliminate the reflected waves from the coaxial cylinders and to act as matching load. Additionally, the smooth transition area between the inner conductor and the top connection point of the filtenna is designed to ensure impedance matching. The electric field of the filtenna indicates that the majority of the power is radiated from the resonant slots, with only a minimal amount remaining at the bottom. Consequently, these structures improve the efficiency of the filtenna, producing good traveling wave properties and AR results.

3.2 Simulated and Measured Results

The omnidirectional CP filtenna was simulated and optimized using HFSS software. The optimized geometric parameters are summarized in Tab. 3 and a prototype was fabricated and tested, as shown in Fig. 7(a). The simulated

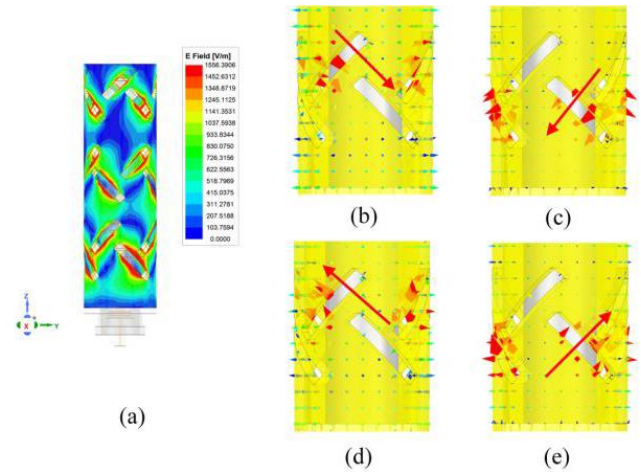


Fig. 6. Electric filed behavior on the sleeve of the filtenna over one period at 9 GHz. (a) Electric field distribution. (b) $t = 0$. (c) $t = T/4$. (d) $t = 2T/4$. (e) $t = 3T/4$.

and measured S-parameters are shown in Fig. 7(b), indicating that the measured impedance bandwidth of $S_{11} < -10$ dB is 5.8%. The outcome is in general agreement with the results of the simulation but slightly deflected to the high frequency. There is a probability that the actual permittivity constant value ϵ_r is smaller than the simulated value of $\epsilon_r = 2.1$ due to the impurity of the teflon medium. Figure 8 demonstrates the measured average AR and gain in the xy-plane. The measured AR bandwidth of less than 3 dB is 6.1%, ranging from 8.85 to 9.4 GHz, while the measured gain is better than 5.29 dBic from 8.87 GHz to 9.39 GHz demonstrating the same trend as the simulated ones. The proposed filtenna obtains the stable high gain within the AR bandwidth.

Symbol	Value	Symbol	Value
D_1	26	L_4	29.5
D_2	14	S_1	15.8
D_3	6.6	W_1	3.0
D_4	2.6	S_2	15.8
T_1	2.0	W_2	3.0
T_2	2.0	S_3	15.8
T_3	3.0	W_3	3.0
L_1	4.06	Z_1	11.74
L_2	28.7	Z_2	12.02
L_3	27.5	Z_3	12.02

Tab. 3. Optimized geometric parameter of the CP filtenna (in mm).

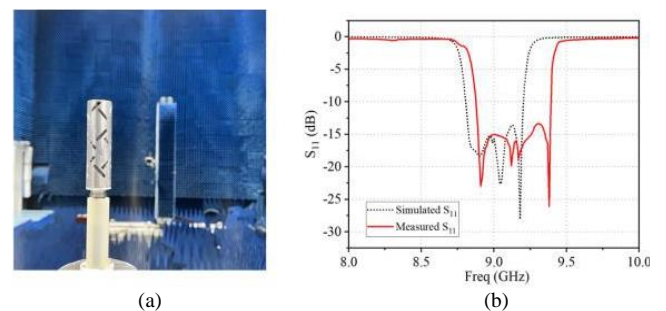


Fig. 7 (a) Photography of the filtenna fabricated. (b) Comparison of the simulated and measured S_{11} of the filtenna.

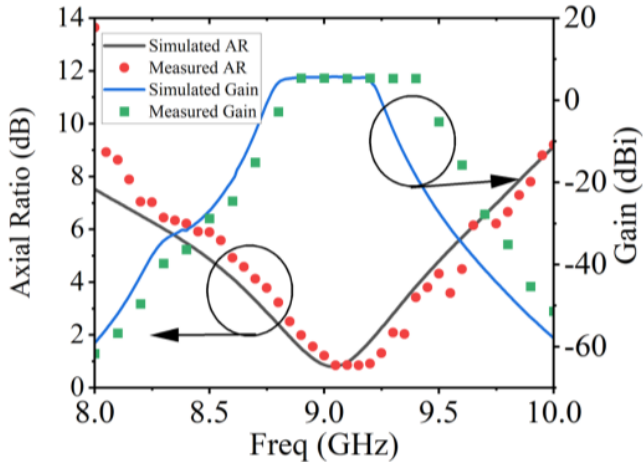


Fig. 8. Comparison of the simulated and measured realized gain and AR.

The measured LHCP normalized radiation patterns and simulated RHCP and LHCP normalized radiation patterns in the yz -plane and xy -plane (omnidirectional plane) at 8.8 GHz, 9 GHz and 9.2 GHz are shown in Fig. 9. Simulated results indicate that the cross-polarization levels are more than 16 dB lower than the co-polarization, and the measured results show reasonable agreement with these simulations. At 9 GHz, the FNBW value of the main lobe are 15 and 22 degrees, respectively. The energy contained within the main lobe is about 58.8%.

Table 4 presents the performance comparison between the proposed filtenna and other designs. The table reveals that the gain of low-profile filtennas in [14, 15, 17, 28, 29] are worse than the prototype, and the antennas mentioned in [14, 15, 26, 28, 29] also have difficulty in achieving circular polarization characteristics. The antenna in [30] lacks filtering. Consequently, the proposed filtenna has superior overall performance in terms of compact structure, filtering function and CP characteristics.

4. Conclusion

A slot array filtenna on a coaxial cylinder with omnidirectional CP radiation is proposed. The realization of the filtering properties is implemented based on a tubular filter

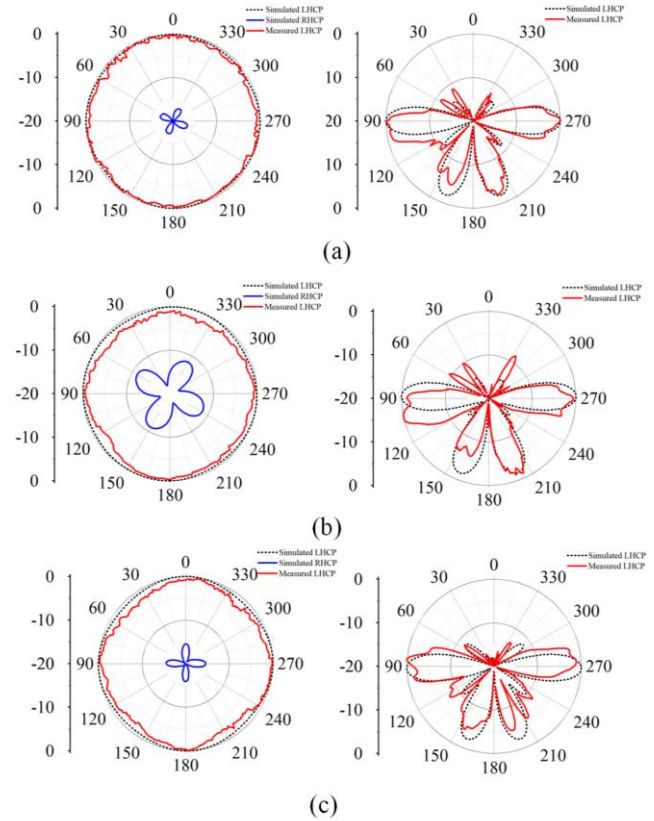


Fig. 9. Simulated RHCP and LHCP and measured normalized radiation pattern in the omnidirectional plane (xy -plane on the left) and the E-plane (yz -plane on the right). (a) 9 GHz; (b) 8.8 GHz; (c) 9.2 GHz.

which consists of the high and low impedance transformations of the conductor within the coaxial waveguide, along with insertion of the dielectric disk. The fabricated prototype's measured results are generally consistent with the simulated results. The prototype exhibits a -10 dB impedance bandwidth of 5.8% and a 3 dB AR bandwidth of 6.1%. The measured gain is better than 5.29 dBic in the operating bandwidth from 8.87 GHz to 9.39 GHz. The proposed filtenna demonstrates excellent performance in omnidirectional characteristic, with an out-of-roundness of less than 1.5 dB in the radiation direction. In terms of miniaturization, the overall size of the filtenna is $0.78\lambda_0 \times 3.04\lambda_0$.

Ref.	Polarization	Center Freq. (GHz)	3dB Axial Ratio Bandwidth	Dimensions (λ_0)	Gain (dBi)	Filtering
[14]	linear	2.9	-	$0.33 \times 0.32 \times 0.007$	2.5	Yes
[15]	linear	4.9/5.2	-	$0.21 \times 0.37 \times 0.007$	2.5	Yes
[17]	circular	2.45	20%	$0.57 \times 0.61 \times 0.007$	3.3	Yes
[26]	linear	4.5	-	$1.1 \times 1.1 \times 0.029$	6.0	Yes
[28]	linear	1.65	-	$1.41 \times 0.76 \times 0.007$	2.4	Yes
[29]	linear	2.354	-	$0.36 \times 0.64 \times 0.007$	1.15	Yes
[30]	circular	5.5	14.5%	$2.43 \times 2.43 \times 1.0$	5.8	No
[38]	linear	2.8	-	$0.33 \times 0.33 \times 1.52$	6.6	Yes
This	circular	9.13	6.1%	$0.78 \times 0.78 \times 2.91$	6.5	Yes

Tab. 4. Comparison of the performance of the CP omnidirectional filter antenna designed in this paper with related literature.

Acknowledgments

This work was funded by projects including the Scientific Research Foundation for the Highlevel Personnel of Nanjing Institute of Technology (grant: YKJ2019109).

References

- [1] LUO, Y., CHEN, Z. N., MA, K. Enhanced bandwidth and directivity of a dual-mode compressed high-order mode stub-loaded dipole using characteristic mode analysis. *IEEE Transactions on Antennas and Propagation*, 2019, vol. 67, no. 3, p. 1922–1925. DOI: 10.1109/TAP.2018.2889025
- [2] YANG, Y., LI, Z., WANG, S., et al. Miniaturized high-order-mode dipole antennas based on spoof surface plasmon polaritons. *IEEE Antennas and Wireless Propagation Letters*, 2018, vol. 17, no. 12, p. 2409–2413. DOI: 10.1109/LAWP.2018.2876691
- [3] WEN, D., HAO, Y., WANG, H., et al. Design of a wideband antenna with stable omnidirectional radiation pattern using the theory of characteristic modes. *IEEE Transactions on Antennas and Propagation*, 2017, vol. 65, no. 5, p. 2671–2676. DOI: 10.1109/TAP.2017.2679767
- [4] MA, Z. L. Inductively loaded segmented loop antenna by using multiple radiators. *IEEE Antennas and Wireless Propagation Letters*, 2017, vol. 16, p. 109–112. DOI: 10.1109/LAWP.2016.2558544
- [5] WU, J., SARABANDI, K. Compact omnidirectional circularly polarized antenna. *IEEE Transactions on Antennas and Propagation*, 2017, vol. 65, no. 4, p. 1550–1557. DOI: 10.1109/TAP.2017.2669959
- [6] LIU, J., XUE, Q., WONG, H., et al. Design and analysis of a low-profile and broadband microstrip monopolar patch antenna. *IEEE Transactions on Antennas and Propagation*, 2013, vol. 61, no. 1, p. 11–18. DOI: 10.1109/TAP.2012.2214996
- [7] WEN, S., DONG, Y. A low-profile wideband antenna with monopolelike radiation characteristics for 4g/5g indoor micro base station application. *IEEE Antennas and Wireless Propagation Letters*, 2020, vol. 19, no. 12, p. 2305–2309. DOI: 10.1109/LAWP.2020.3030968
- [8] LIN, S., LIAO, S., YANG, Y., et al. Gain enhancement of low-profile omnidirectional antenna using annular magnetic dipole directors. *IEEE Antennas and Wireless Propagation Letters*, 2021, vol. 20, no. 1, p. 8–12. DOI: 10.1109/LAWP.2020.3035819
- [9] CAO, Y. F., CHEUNG, S. W., YUK, T. I. A multiband slot antenna for GPS/WiMAX/WLAN systems. *IEEE Transactions on Antennas and Propagation*, 2015, vol. 63, no. 3, p. 952–958. DOI: 10.1109/TAP.2015.2389219
- [10] LU, W. J., ZHU, L. Wideband stub-loaded slotline antennas under multi-mode resonance operation. *IEEE Transactions on Antennas and Propagation*, 2015, vol. 63, no. 2, p. 818–823. DOI: 10.1109/TAP.2014.2379921
- [11] ZHANG, Y., ZHANG, X. Y., PAN, Y. M. Compact single- and dual-band filtering patch antenna arrays using novel feeding scheme. *IEEE Transactions on Antennas and Propagation*, 2017, vol. 65, no. 8, p. 4057–4066. DOI: 10.1109/TAP.2017.2717046
- [12] ZHANG, X. Y., ZHANG, Y., PAN, Y. M., et al. Low-profile dual-band filtering patch antenna and its application to LTE MIMO system. *IEEE Transactions on Antennas and Propagation*, 2017, vol. 65, no. 1, p. 103–113. DOI: 10.1109/TAP.2016.2631218
- [13] SAKAGUCHI, K., HASEBE, N. A circularly polarized omnidirectional antenna. In *Proceedings of 1993 Eighth International Conference on Antennas and Propagation*. Edinburgh (UK), 1993, p. 477–480. ISBN: 0-85296-572-9
- [14] SUN, G. H., WONG, S. W., ZHU, L., et al. A compact printed filtering antenna with good suppression of upper harmonic band. *IEEE Antennas and Wireless Propagation Letters*, 2016, vol. 15, p. 1349–1352. DOI: 10.1109/LAWP.2015.2508918
- [15] HU, H. T., CHEN, F. C., CHU, Q. X. Novel broadband filtering slotline antennas excited by multimode resonators. *IEEE Antennas and Wireless Propagation Letters*, 2017, vol. 16, p. 489–492. DOI: 10.1109/LAWP.2016.2585524
- [16] SOLTANPOUR, M., FAKHARIAN, M. M. Compact filtering slot antenna with frequency agility for Wi-Fi/LTE mobile applications. *Electronics Letters*, 2016, vol. 52, no. 7, p. 491–492. DOI: 10.1049/el.2015.3198
- [17] CHENG, W., LI, D. Circularly polarised filtering monopole antenna based on miniaturised coupled filter. *Electronics Letters*, 2017, vol. 53, no. 11, p. 700–702. DOI: 10.1049/el.2017.1094
- [18] CHEN, X., ZHAO, F., YAN, L., et al. A compact filtering antenna with flat gain response within the passband. *IEEE Antennas and Wireless Propagation Letters*, 2013, vol. 12, p. 857–860. DOI: 10.1109/LAWP.2013.2271972
- [19] FAKHARIAN, M. M., REZAEI, P., OROUJI, A. A., et al. A wideband and reconfigurable filtering slot antenna. *IEEE Antennas and Wireless Propagation Letters*, 2016, vol. 15, p. 1610–1613. DOI: 10.1109/LAWP.2016.2518859
- [20] TANG, M. C., WANG, H., DENG, T., et al. Compact planar ultrawideband antennas with continuously tunable, independent band-notched filters. *IEEE Transactions on Antennas and Propagation*, 2016, vol. 64, no. 8, p. 3292–3301. DOI: 10.1109/TAP.2016.2570254
- [21] AGHDAM, S. A. Reconfigurable antenna with a diversity filtering band feature utilizing active devices for communication systems. *IEEE Transactions on Antennas and Propagation*, 2013, vol. 61, no. 10, p. 5223–5228. DOI: 10.1109/TAP.2013.2273812
- [22] ZHANG, Y., ZHANG, X. Y., PAN, Y. M. Low-profile planar filtering dipole antenna with omnidirectional radiation pattern. *IEEE Transactions on Antennas and Propagation*, 2018, vol. 66, no. 3, p. 1124–1132. DOI: 10.1109/TAP.2018.2790169
- [23] HU, P. F., PAN, Y. M., LEUNG, K. W., et al. Wide-/dual-band omnidirectional filtering dielectric resonator antennas. *IEEE Transactions on Antennas and Propagation*, 2018, vol. 66, no. 5, p. 2622–2627. DOI: 10.1109/TAP.2018.2809706
- [24] HU, P. F., PAN, Y. M., ZHANG, X. Y., et al. A compact filtering dielectric resonator antenna with wide bandwidth and high gain. *IEEE Transactions on Antennas and Propagation*, 2016, vol. 64, no. 8, p. 3645–3651. DOI: 10.1109/TAP.2016.2565733
- [25] HU, P. F., PAN, Y. M., ZHANG, X. Y., et al. Broadband filtering dielectric resonator antenna with wide stopband. *IEEE Transactions on Antennas and Propagation*, 2017, vol. 65, no. 4, p. 2079–2084. DOI: 10.1109/TAP.2017.2670438
- [26] WU, T. L., PAN, Y. M., HU, P. F., et al. Design of a low profile and compact omnidirectional filtering patch antenna. *IEEE Access*, 2017, vol. 5, p. 1083–1089. DOI: 10.1109/ACCESS.2017.2651143
- [27] PAL, P., SINHA, R., KUMAR MAHTO, S. A compact wideband circularly polarized planar filtenna using synthesis technique for 5 GHz WLAN application. *AEU - International Journal of Electronics and Communications*, 2022, vol. 148, p. 1–9. DOI: 10.1016/j.aeu.2022.154180
- [28] ZHANG, G., WANG, J., WU, W. Wideband balun bandpass filter explored for a balanced dipole antenna with high selectivity. *Electronics Letters*, 2016, vol. 52, no. 13, p. 1153–1155. DOI: 10.1049/el.2016.0716

- [29] TANG, M. C., CHEN, Y., ZIOLKOWSKI, R. W. Experimentally validated, planar, wideband, electrically small, monopole filtennas based on capacitively loaded loop resonators. *IEEE Transactions on Antennas and Propagation*, 2016, vol. 64, no. 8, p. 3353–3360. DOI: 10.1109/TAP.2016.2576499
- [30] ZHOU, B., GENG, J., BAI, X., et al. An omnidirectional circularly polarized slot array antenna with high gain in a wide bandwidth. *IEEE Antennas and Wireless Propagation Letters*, 2015, vol. 14, p. 666–669. DOI: 10.1109/LAWP.2014.2376961
- [31] CHENHU, G., GENG, J., ZHOU, H., et al. Truncated circular cone slot antenna array that radiates a circularly polarized conical beam. *IEEE Antennas and Wireless Propagation Letters*, 2017, vol. 16, p. 2574–2577. DOI: 10.1109/LAWP.2017.2734820
- [32] SU, T., WU, B., LIANG, C.-H. The designing and tuning methods of tubular filter. In *Proceedings of 2005 Asia-Pacific Microwave Conference Proceedings*. Suzhou (China), 2005, p. 1–3. DOI: 10.1109/APMC.2005.1607030
- [33] WU, B., SU, T., LI, B., et al. Design of tubular filter based on curve-fitting method. *Journal of Electromagnetic Waves and Applications*, 2006, vol. 20, no. 8, p. 1071–1080. DOI: 10.1163/156939306776930231
- [34] MEJILLONES, S. C., OLDONI, M., MOSCATO, S., et al. Circularly polarized coaxial horn filtenna for electromagnetic interference mitigation. *IEEE Transactions on Antennas and Propagation*, 2023, vol. 71, no. 12, p. 9487–9496. DOI: 10.1109/TAP.2023.3321422
- [35] BARBUTO, M., TROTTA, F., BILOTTI, F., et al. Design and experimental validation of dual-band circularly polarised horn filtenna. *Electronics Letters*, 2017, vol. 53, no. 10, p. 641–642. DOI: 10.1049/el.2017.0145
- [36] BARBUTO, M., TROTTA, F., BILOTTI, F., et al. Filtering chiral particle for rotating the polarization state of antennas and waveguides components. *IEEE Transactions on Antennas and Propagation*, 2017, vol. 65, no. 3, p. 1468–1471. DOI: 10.1109/TAP.2016.2640143
- [37] KUMAR CHOUDHARY, D., KUMAR CHAUDHARY, R. Compact filtering antenna using asymmetric CPW-fed based CRLH structure. *AEU - International Journal of Electronics and Communications*, 2020, vol. 126, p. 1–6. DOI: 10.1016/j.aeue.2020.153462
- [38] ZHANG, S. Q., WONG, S. W., ZHANG, Z., et al. Full-metal omnidirectional filtenna array using 3-D metal printing technology. *IEEE Transactions on Antennas and Propagation*, 2024, vol. 72, no. 5, p. 4095–4106. DOI: 10.1109/TAP.2024.3385914

About the Authors ...

Duo ZHANG received the Ph.D. degree in Microwave Engineering from Nanjing University of Science & Technology in 2018. Currently, he is working at Nanjing Institute of Technology from 2019. His research interests include microwave circuit design and radar system research.

Keren ZHU received the Ph.D. degree in Microwave Engineering from Nanjing University of Science & Technology in 2023. His research interests include microwave circuit design and radar system research.

Shishan QI (corresponding author) received the Ph.D. degree in Electromagnetic Field and Microwave Technology from Nanjing University of Science & Technology in 2012. Currently, he is working at Nanjing University of Science & Technology from 2012. His research interests include microwave antenna theory and radar system research.